



## Non-destructive Detection for the Early Drought Stress Status of Tomato (*Solanum lycopersicum*) by Spectroscopy and Deep Learning

Crop Genetic Resource and Biotechnology Division  
Taiwan Agricultural Research Institute (TARI)  
Yuan Kai, Tu. Ph.D.



## Personal information

### Education

- Ph.D., Department of Agronomy, National Chung-Hsing University, Taiwan.
- M.S., Graduate Institute of Biochemical Science, National Taiwan University, Taiwan.
- B.S., Department of Science Education, University of Taipei, Taiwan.



### Working Experience and Training

- 2023: Associate Researcher, Biotechnology Division, Taiwan Agricultural Research Institute.
- 2023: Summer School on Image Analysis for Plant Phenotyping. Wageningen University and Research. Nederland.
- 2018: Visiting Scholar. Australian Plant Phenomics Facility (APPF). Australia.
- 2017: Machine Learning for Big Visual Data. IEEE International Elite School. Taiwan.



## Outline

- Challenge of tomato (*Solanum lycopersicum*) cultivation.
- Aim
- Deep learning
- Experiment design:
  - ✓ Greenhouse experiment
  - ✓ Model building and evaluation
- Results
- Conclusions



## Challenge of tomato cultivation in Taiwan

Zhou et al. *BMC Plant Biology* (2017) 17:24  
DOI 10.1186/s12870-017-0974-x

BMC Plant Biology

RESEARCH ARTICLE

Open Access

To pr



### Drought stress had a predominant effect over heat stress on three tomato cultivars subjected to combined stress



Rong Zhou<sup>1,2,3†</sup>, Xiqing Yu<sup>3†</sup>, Carl-Otto Otosen<sup>4</sup>, Eva Rosenqvist<sup>5</sup>, Liping Zhao<sup>1,2</sup>, Wei Wang<sup>1</sup>, Wenqin Xu<sup>1</sup>, Tongmin Zhao<sup>1,2\*</sup> and Zhen Wu<sup>3\*</sup>

High Temp → Heat stress  
Drought stress



Plant height and leaf growth parameters of the three tomato cultivars under four days of control, drought, heat and combined stress. Different sub-graphs represent three tomato cultivars and phenotypes of 'Arvento', 'LA1994' and 'LA2093' under control, drought, heat and combined stress. The data represent mean values  $\pm$  SE (n = 4). Different small letters above the bars indicate significant differences ( $p < 0.05$ )



## Tomato drought stresses



Weak growth



Flowers and fruits dropping



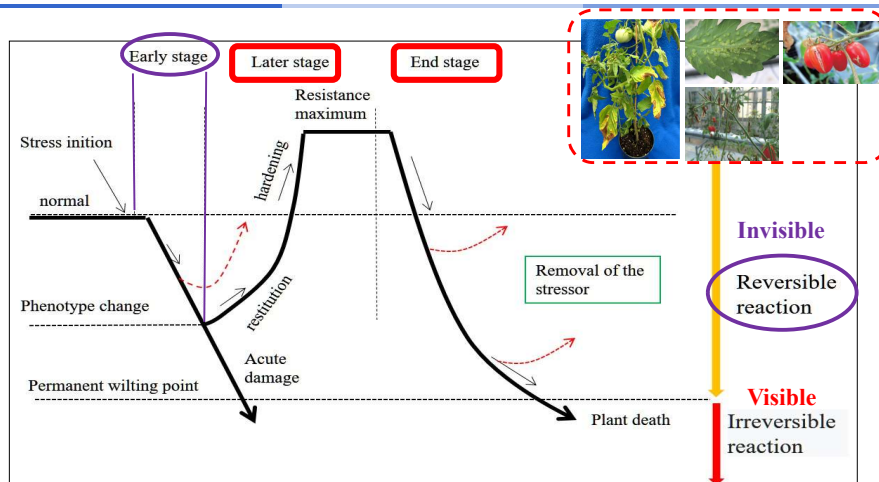
Fruit cracking.



Odema



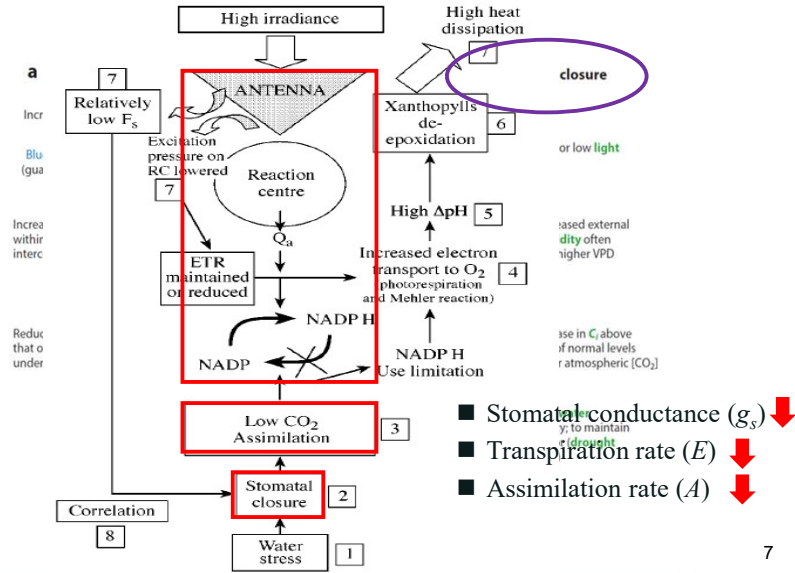
## Early physiological status under drought stress



Physiological responses and state changes of plants after encountering drought stress. (modified from Lichtenthaler, 1998) ◦



## Early physiological alteration under drought stress



## Physiological indicators of early drought status

- Stomatal conductance ( $g_s$ ) ↓
- Transpiration rate ( $E$ ) ↓
- Assimilation rate ( $A$ ) ↓

Invisible Reversible

Visible Irreversible

Early drought status

Middle and late

Drought stress

Drought treatment →

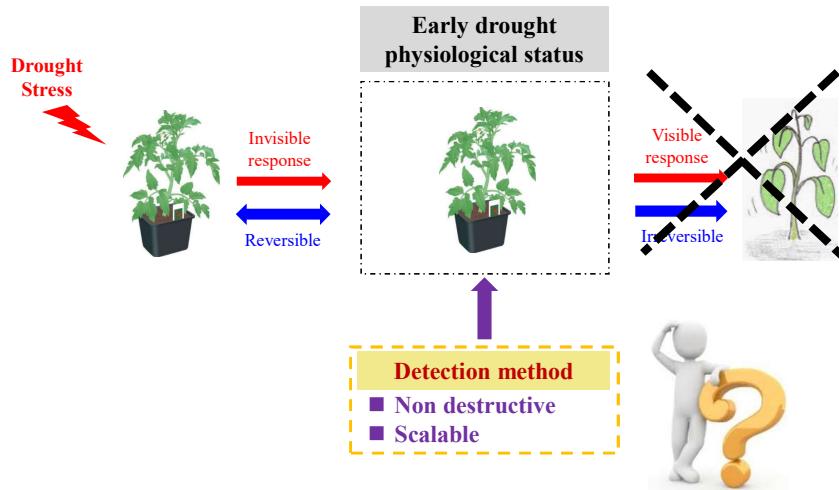


Recoverable

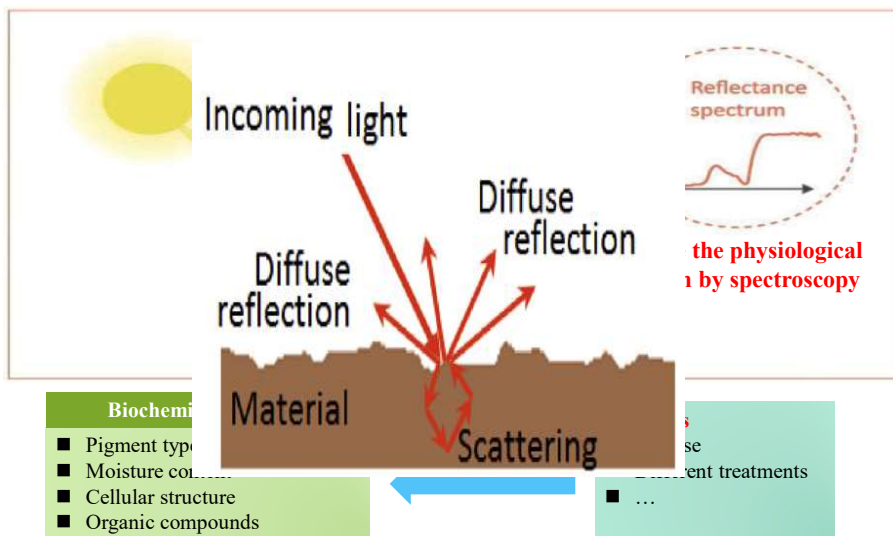
Irrecoverable



## Aim

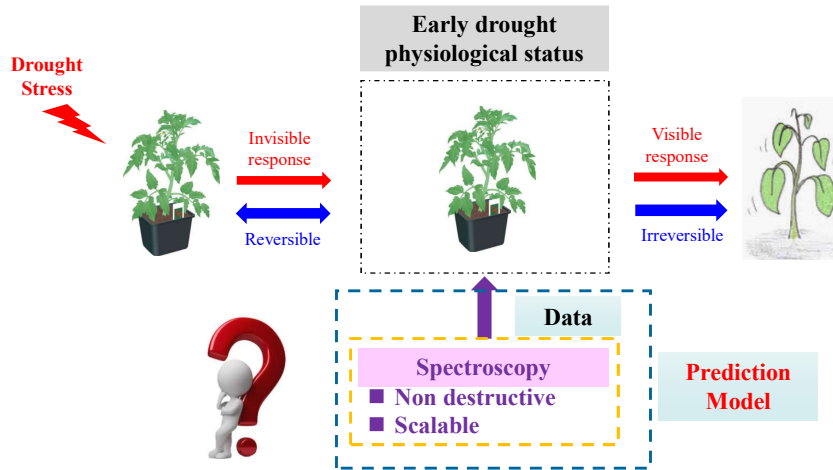


## Spectroscopy vs Physiological response

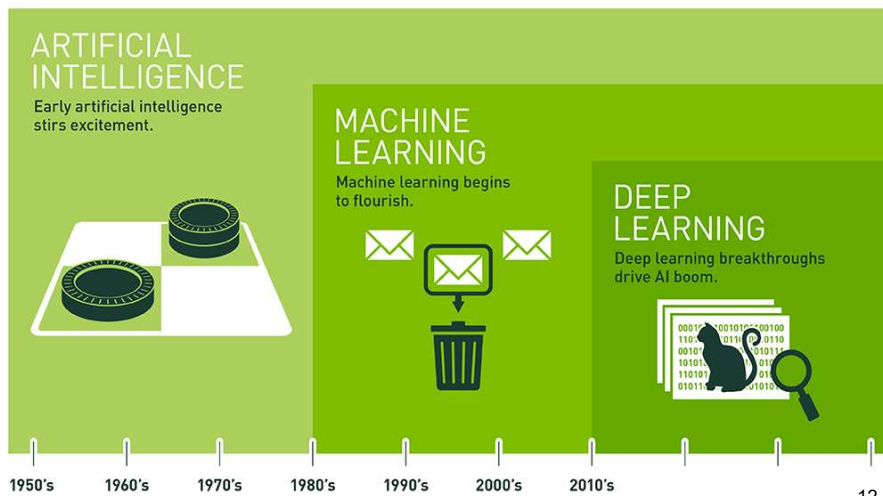




## Aim



## Deep learning





**(a) Variety classification**

Classification of fruit and vegetable  
Classification of KVM seeds  
Classification of rice variety  
Classification of tea species

**(b) Ripeness and content prediction**

Prediction of ripeness and soluble solid content of guava and kiwifruit  
Detection of spinach freshness  
Prediction of chlorophyll content in lettuce leaves

**Deep learning in agriculture:**

- Classification
- Prediction
- Detection
- Segmentation

**(c) Remote sensing image classification**

Legend:  
- Apple  
- Maize  
- Rice  
- Pasture  
- Forest  
- Water  
- Urban  
- Bare field  
- Road  
- Shadow  
- Cloud  
- Snow

**(d) Plant disease detection**

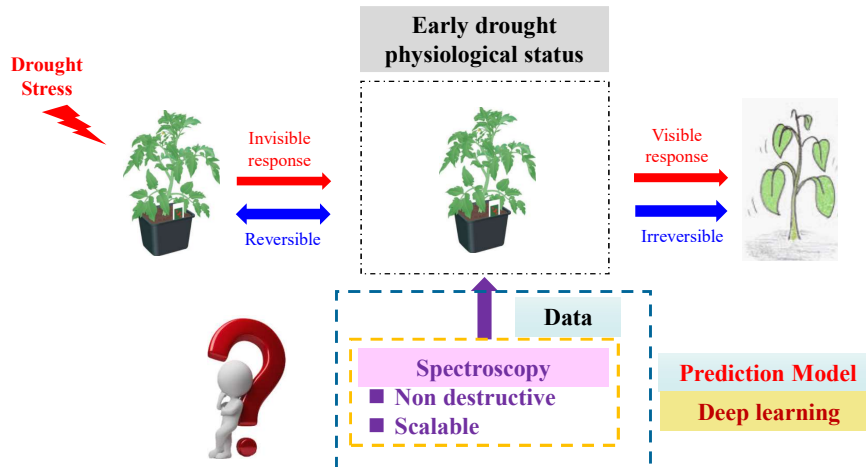
Detection of watermelon spots  
Classification of citrus fruit diseases  
Detection of green potato  
Detection of soybean leaf diseases  
Detection of alfalfa root rot



Semantic segmentation of the fruits.



**Aim**





## Experiment design

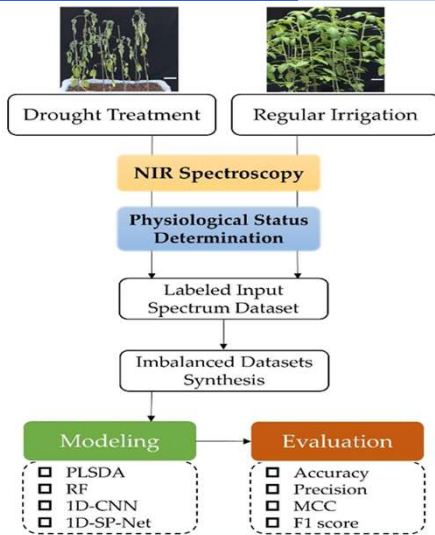
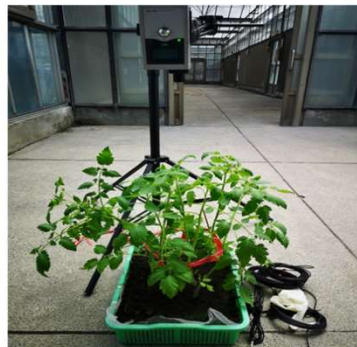


**Figure 1.** General workflow in this study. NIR, near infrared; PLSDA, partial least squares discriminant analysis; RF, random forest; 1D-CNN, one-dimensional convolutional neural network; 1D-SP-Net, one-dimensional spectrogram power net; MCC, Matthew's correlation coefficient.



## Data collection

- Cherry tomato: 'Yu Nu'.
- LI-6800 Portable Photosynthesis System.
- MS-720 Portable Spectroradiometer.
- WaterScout SM100.

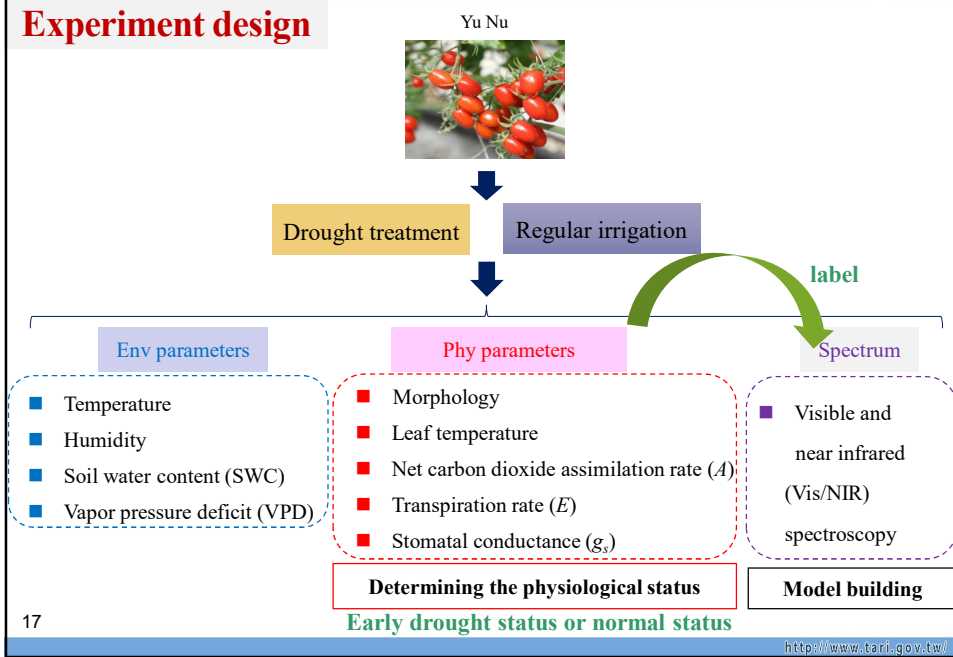


Demonstration of environmental, physiological and NIR spectrum data collection by portable photosynthesis system LI-6800 (left) and spectroradiometer MS-720 (right).



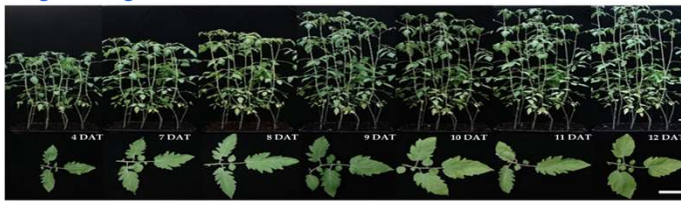


## Experiment design



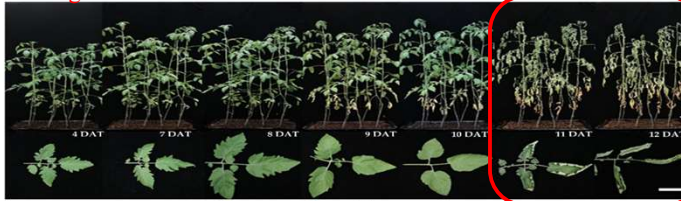
## Results

### Regular irrigation



(a)

### Drought treatment



(b)

Significant branch softening and drooping, leaves softened and heavily curled up with leaves.

**Figure 2.** Morphological alterations from 4 to 12 days after treatment (DAT) in different treatment groups: (a) regular irrigation treatment and (b) drought treatment (bar = 5 cm).



### Results

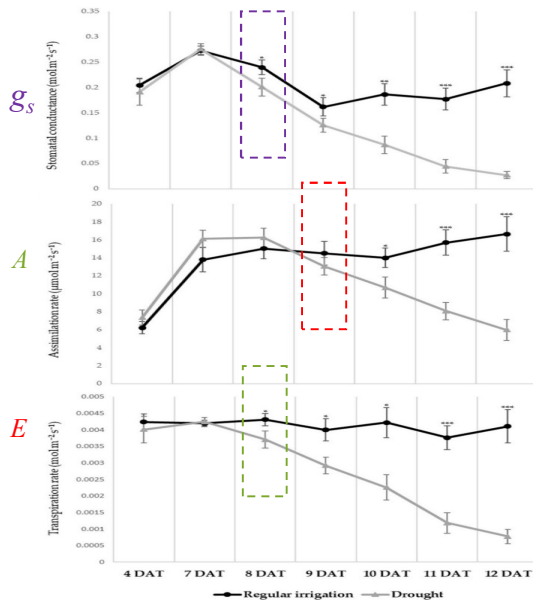
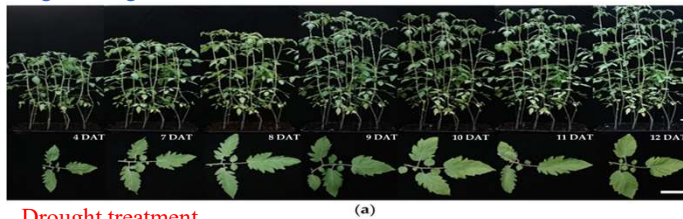


**Figure 3.** Stomatal conductance ( $g_s$ ), transpiration rate ( $E$ ), and assimilation rate ( $A$ ) changes under regular irrigation treatment and drought treatment from 4 to 12 DAT. Differences are represented as significant (\*), highly significant (\*\*), and extremely significant (\*\*\*) at the 5%, 1%, and 0.1% levels, respectively, as determined by Student's t test. The error bar indicates the standard deviation.



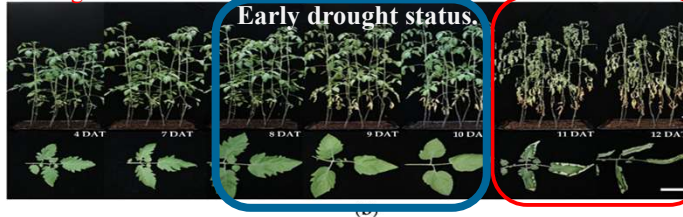
### Results

#### Regular irrigation



(a)

#### Drought treatment



Later and end status.

**Figure 2.** Morphological alterations from 4 to 12 days after treatment (DAT) in different treatment groups: (a) regular irrigation treatment and (b) drought treatment (bar = 5 cm).



## Results

- Normal physiological status: There are **246** entries marked as '0'
- Early drought status: **132** entries marked as '1'

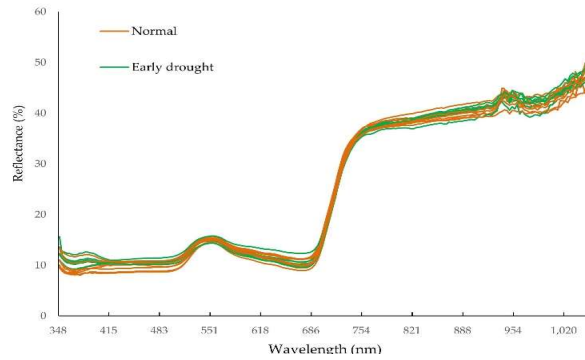
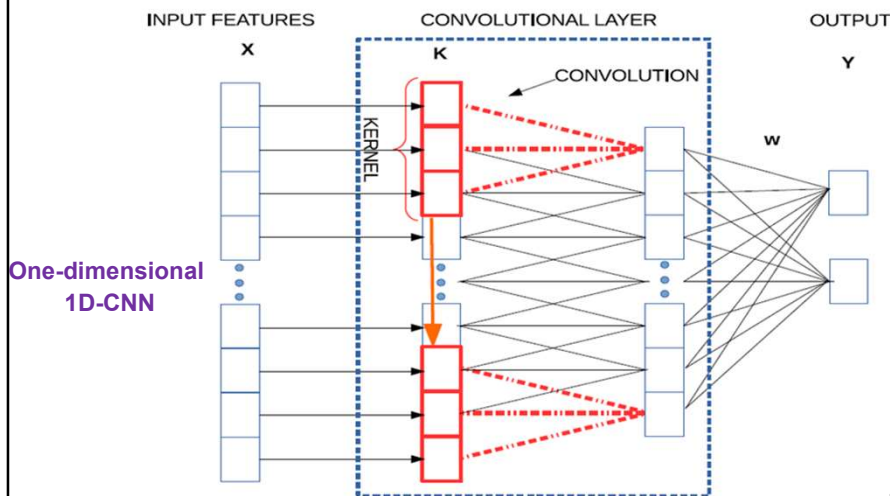


Figure 3. NIR spectra of “normal physiological status” (brown line) and “early physiological drought status” (green line) for the tomato variety “Rosada.” °



## Convolutional neural network (CNN)





### Model building – 1DCNN

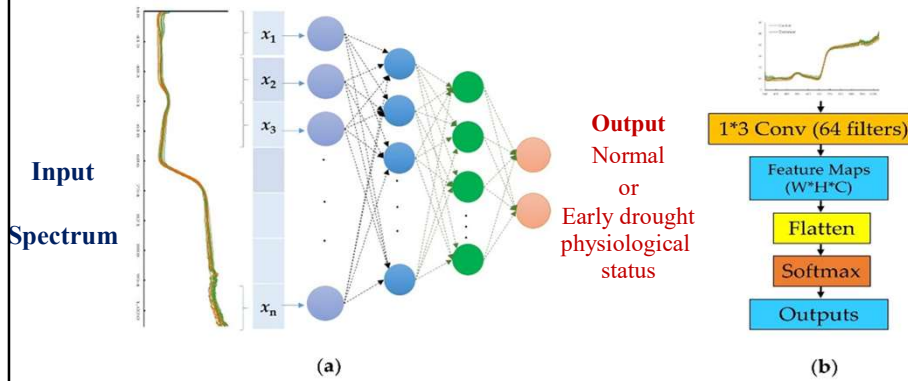


**Figure 4.** Illustration of the 1D-CNN (**one-dimensional convolutional neural network, 1D-CNN**): (a). The network comprised an input layer (light purple circles) transformed from the input spectra (far left), a feature layer (blue circles), a fully connected layer (green circles) and an output layer (orange circles) that represented the classification results (“normal” or “early drought stress” physiological status); (b). hierarchical layer flow of the 1D-CNN model. W, H and C represent the width, height, and number of channels of the feature map, respectively.



### Model building – 1D-SP-Net

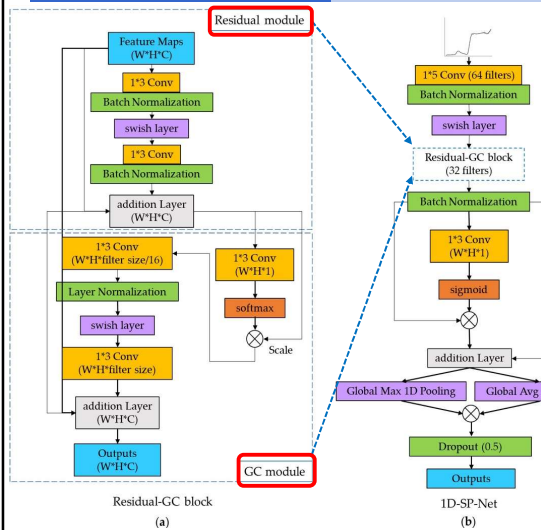


**Figure 5.** Architecture of the proposed 1D-SP-Net: (a) residual block and global context (GC) block; (b) hierarchical structure of the 1D-SP-Net.

- The **Residue module** has the characteristics of **reducing training errors** and **simplifying the operation process** (He et al., 2016)
- The **GC module** has the feature of self attention learning, which can enhance the ability to **extract global and local features**.
- Zhao et al. (2021) demonstrated that the prediction accuracy of the CNN model can also be improved to 96.0%



## Results

**Table 1.** Comparison of predictive performance for PLSDA, RF, 1D-CNN, and 1D-SP-Net models by accuracy, precision, MCC, and F1 score metrics.

Model	Training				Testing			
	Accuracy (%)	Precision (%)	MCC	F1 score	Accuracy (%)	Precision (%)	MCC	F1 score
PLSDA	93.2	90.4	0.85	0.90	86.7	82.9	0.70	0.80
RF	81.1	75.6	0.58	0.71	77.2	68.4	0.49	0.67
1D-CNN	90.0	88.0	0.79	0.87	90.0	80.0	0.74	0.80
1D-SP-Net	<b>96.0<sup>a</sup></b>	<b>93.1</b>	<b>0.91</b>	<b>0.94</b>	<b>96.3</b>	<b>98.0</b>	<b>0.92</b>	<b>0.95</b>

<sup>a</sup> Bold characters represent the highest values for a respective metric among the models.

**1D-SP-Net > PLSDA = 1D-CNN > RF**



## Results

Lower performance in testing results. **Overfitting.**

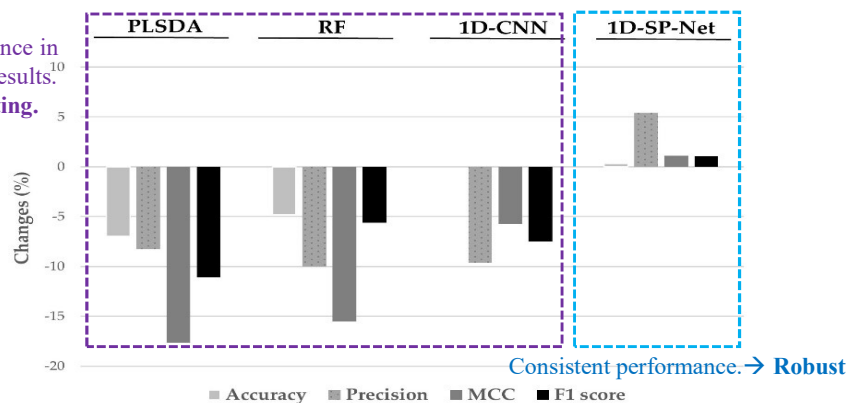


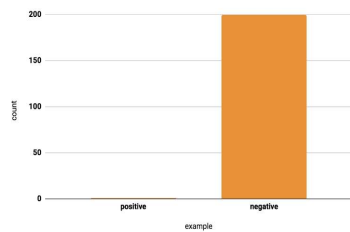
**Figure 6.** Changes (%) of performance in accuracy, precision, MCC (Matthew's correlation coefficient) and F1 scores between training and testing results of the PLSDA (partial least squares discriminant analysis), RF (random forest), 1D-CNN (one-dimensional convolutional neural network) and 1D-SP-Net (one-dimensional spectrogram power net) models.



### Issue of class imbalance

→ A classification data set with skewed class proportions.

- Negative to model performance (Lee *et al.*, 2017).
- CNN models have been applied to deal with classification imbalanced data sets (Buda *et al.*, 2018; Ding *et al.*, 2017; Nemoto *et al.*, 2018).
- Khan *et al.* (2018) confirmed that the model constructed by CNN has better predictive ability.



### Issue of class imbalance

$$\text{Imbalance ratio (IR)} = \frac{\text{Number of major class (Normal physiological status)}}{\text{Number of minor class (Early drought status)}}$$

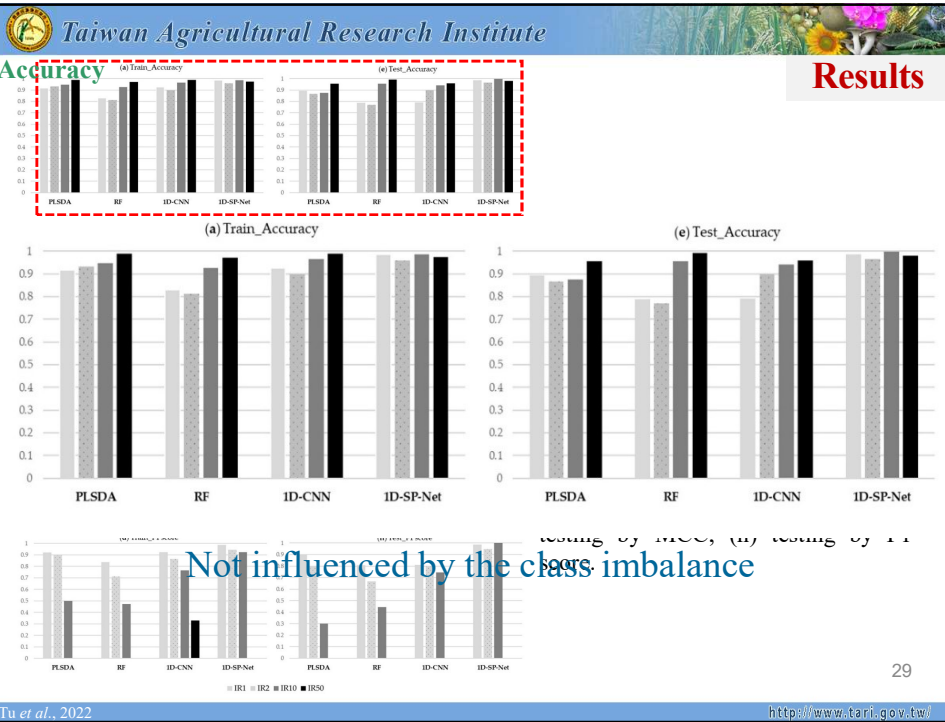
**Table 2.** Extent of the imbalance in the data sets used in this study.

Dataset	Type	Imbalance Ratio	Major class <sup>b</sup>	Minor class <sup>c</sup>
IR1	Synthetic <sup>a</sup>	1	189	189
IR2	Original dataset	2	246	132
IR10	Synthetic	10	340	38
IR50	Synthetic	50	370	8

<sup>a</sup> Synthetic data set was established by random sampling from the original data set.

<sup>b</sup> Number of observations that were classed as "normal physiological status.

<sup>c</sup> Number of observations that were classed as "early physiological drought status.



Taiwan Agricultural Research Institute

30

## Accuracy paradox

- Valverde-Albacete *et al.* (2014) explained that the **accuracy** evaluation index is used to measure the model to predict the unbalanced data set, and **cannot actually reflect the predictive performance of the model**.
- The **MCC** and **F1 score** evaluation indicators can **more faithfully reflect the prediction performance of the model** in predicting different imbalanced data sets under the condition of using imbalanced data sets (Chicco *et al.*, 2021; Pillai *et al.*, 2017)

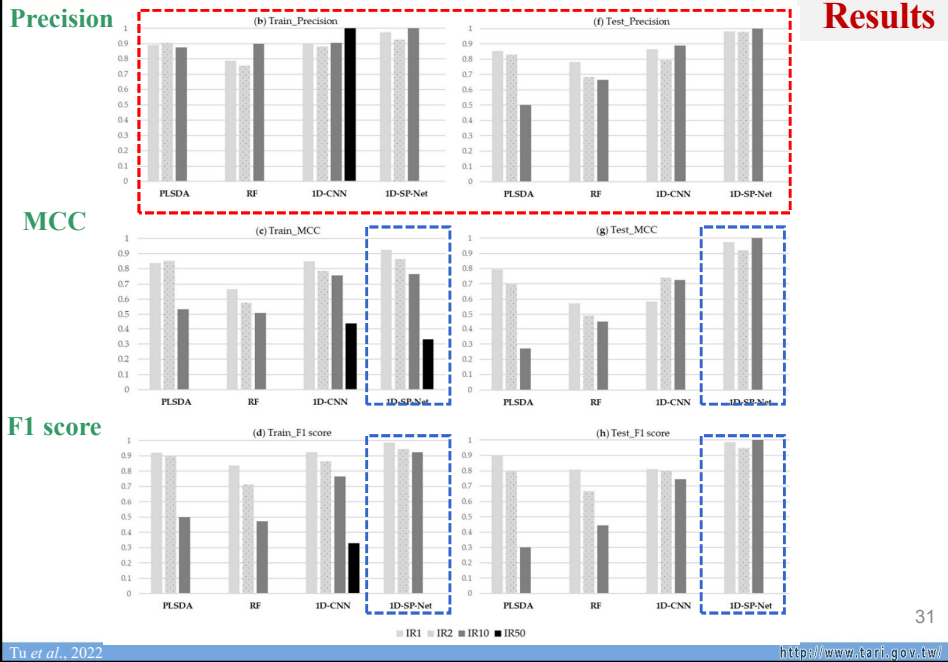
		Distributed <b>unequally</b>		Distributed <b>equally</b>	
		Positive	Negative	Positive	Negative
True condition	Positive	0	0	9	90
	Negative	10	990	1	900

True label class 2

$Acc = \frac{(0+990)}{(0+0+10+990)} = 99\%$ 

 $Acc = \frac{(9+900)}{(9+90+1+900)} = 90.9\%$

<https://www.linkedin.com/pulse/class-imbalance-classification-headache-gonzalo-ferreiro-volpi> <http://www.tari.gov.tw/>



### Conclusions

- The 1D-SP-Net is a promising model that can determine the early drought status of tomato seedlings in a noninvasive manner.
- The 1D-SP-Net is more robust and resistant to the effects of imbalanced data sets than PLSDA, RF, and 1D-CNN models.
- **Key feature bands?**







### Experiment design

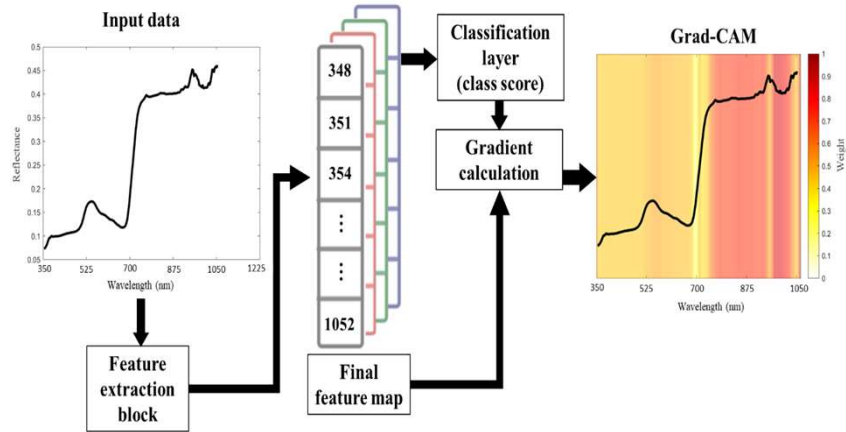
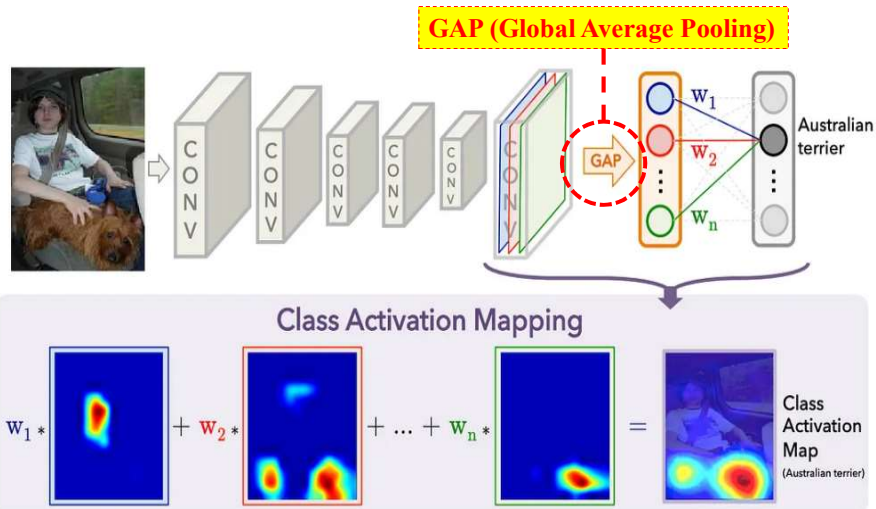


Figure. 8. Flowchart of Grad-CAM (Gradient-weighted class activation mapping ) mechanism for extracting feature bands of spectroscopic data.



### Gradient-weighted class activation mapping (Grad-CAM)





### Results

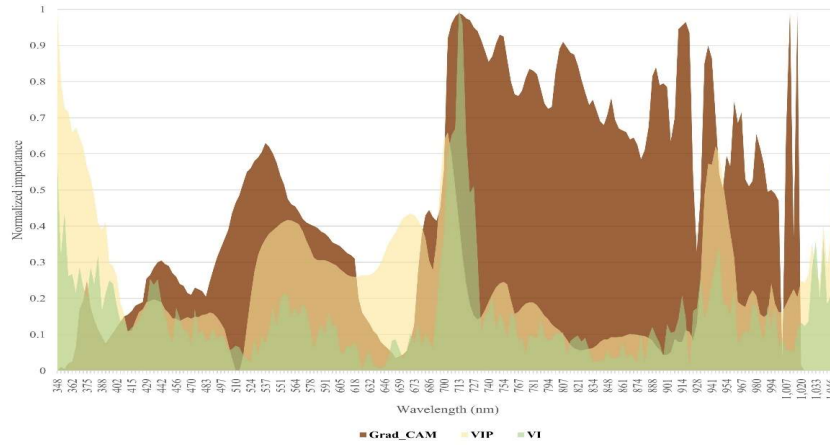


Figure 9. Normalized importance of feature bands for PLSDA (variable importance projection, VIP), RF (variable importance, VI), and 1D-SP-Net (Gradient-weighted class activation mapping, Grad-CAM).



### Results

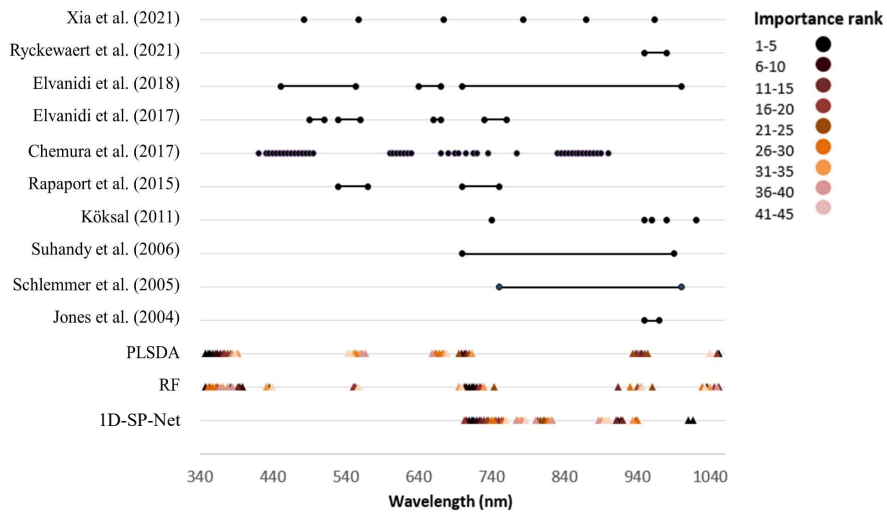


Fig. 10. Distribution of the top 45 ranked feature bands for PLSDA, RF, and 1D-SP-Net. The results of this study are compared with those of previous studies.



### Results

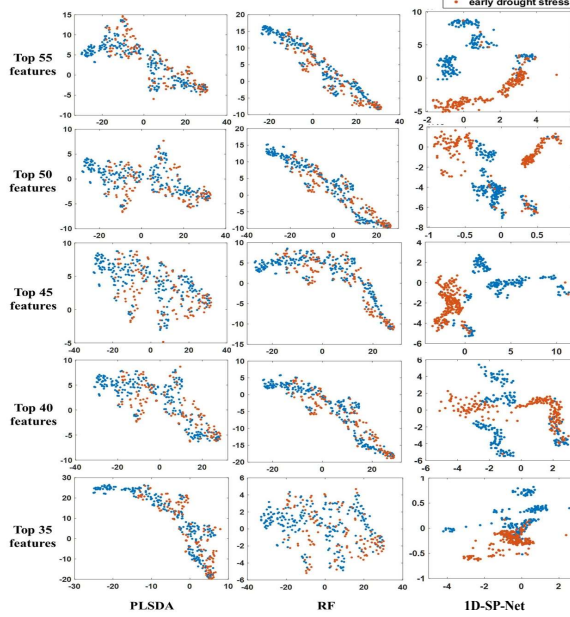


Figure 11. t-SNE (t-distributed stochastic neighbor embedding) maps of various feature groups by ranking (top 55 to top 35 in groups of 5). X axis: feature bands found by VIP of PLS, VI of RF and Grad-CAM of 1D-SP-Net; y axis: number of ranked feature bands.



### Results



Figure 12. Performance of PLSDA, RF, and 1D-SP-Net models when different numbers of features were used. X axis: number of ranked feature bands; y axis: accuracy metric.



## Conclusions

- The 1D-SP-Net is a promising model that can determine the early drought stress status of tomato seedlings in a noninvasive manner
- The 1D-SP-Net is more robust and resistant to the effects of imbalanced data sets than PLSDA, RF, and 1D-CNN models.
- Key feature bands in the Vis/NIR spectroscopic data for 1D-SP-Net were identified using Grad-CAM.
- 1D-SP-Net constructing by less number of feature bands maintain a higher performance.

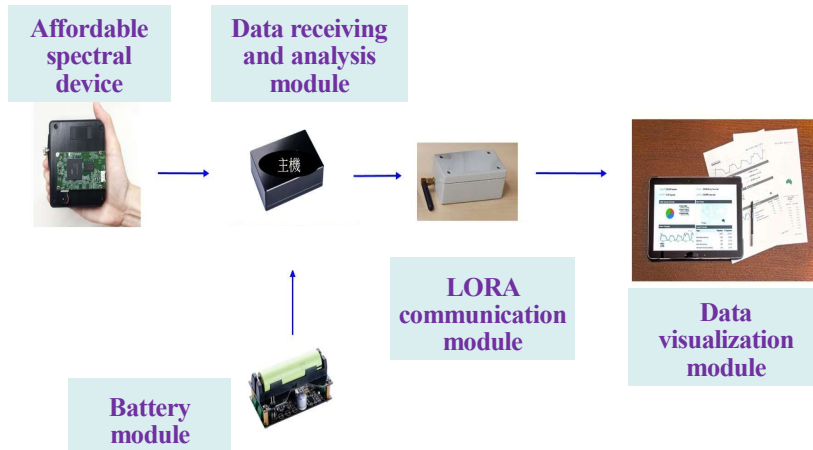


## Ref

- C.E. Kuo, **Y.K. Tu**, S.L. Fang, Y.R. Huang, H.W. Chen, M.H. Yao and B.J. Kuo. Early detection of drought stress in tomato from spectroscopic data: A novel convolutional neural network with feature selection. 2023. Chemometrics and Intelligent Laboratory Systems 293:104869. (Sci) **(Co-First author)**
- S.L. Fang, **Y.K. Tu**, L. Kang, H.W. Chen, T.H. Chang, M.H. Yao and B.J. Kuo. CART model to classify the drought status of diverse tomato geotypes by VPD, air temperature, and leaf-air temperature difference. 2023. Scientific Reports 13:602. (Sci) **(Co-First author)**
- **Y.K. Tu**, C.E. Kuo, S.L. Fang, H.W. Chen, M.K. Chi, M.W. Yao and B.J. Kuo. A 1D-SP-Net to determine early drought stress status of tomato (*Solanum lycopersicum*) with imbalanced Vis/NIR spectroscopy data. 2022. Agriculture 12(2):259. (Sci)
- **Y.K. Tu**, H.W. Chen, M.K. Chi, S.L. Fang, M.W. Yao and B.J. Kuo. Establishment of the Early Prediction Model of Water Deficit Stress for Cherry Tomato Using Hyperspectral Data. 2022. J. Taiwan Agric. Res. 71(2):87-99.
- **Y.K. Tu**, H.W. Chen, S.L. Fang, M.H. Yao and B.J. Kuo. Establishment of early discrimination methods for drought stress of tomato grown in greenhouse by using environmental parameters and NIR spectroscopy. 2020. Acta Hort. 1311:501-512.



## Future work



**Thanks for listening.  
Any comment or question?**